

Experimental Observation of Negative Susceptance in HfO₂-Based RRAM Devices

S. Dueñas, H. Castán, H. García, Óscar G. Ossorio, Luis A. Domínguez,
and E. Miranda, *Senior Member, IEEE*

Abstract—Negative susceptance is experimentally measured in the low resistance state of TiN/Ti/HfO₂/W resistive RAM memories. A meminductive-like behavior appears along with the memristive effects. A detailed study of small-signal parameters measured at 0 V after applying positive and negative voltage pulses is presented. A simple model for the conductive filaments consisting in a resistance in series with an inductance is used. In the equivalent circuit, both elements are in parallel with the geometrical capacitance of the structure. Both resistance and inductance show two clearly differentiate states. Positive voltages switch the device to the ON state, in which the resistance value is low and the inductance value is high. By applying appropriate negative voltages, the device switches to the OFF state, in which resistance value is high and inductance becomes negligible. The negative susceptance could be related to lags between current and electric field due to transport mechanisms occurring in the ON state.

Index Terms—Hafnium oxide, meminductor, MIM capacitor.

I. INTRODUCTION

IN THE last years a great deal of works related to devices that show hysteretic behavior in their current-voltage characteristics has been developed [1]–[4]. They are two-terminal devices of any class whose resistance does not depend on the instantaneous value of the applied voltage, rather on their internal state, and hence they have memory of past states through which have evolved. As they do not lose their state when the electrical power is turned off, they perform as non-volatile memories. These devices were originally predicted to exist by Chua in 1971 by analyzing pairwise relationships between the fundamental quantities of classical circuit theory, and called them memory-resistors (memristors) [5]. The idea was later generalized to a family of dynamical systems called memristive devices [6]. These materials and systems opened new applications, especially for low power

Manuscript received June 19, 2017; revised June 29, 2017; accepted June 29, 2017. Date of publication July 4, 2017; date of current version August 23, 2017. This work was supported by the Spanish Ministry of Economy and Competitiveness through project TEC2014-52152-C3-3-R with the support of Feder funds. The review of this letter was arranged by Editor B. Govoreanu. (*Corresponding author:* S. Dueñas.)

S. Dueñas, H. Castán, H. García, Ó. G. Ossorio, and L. A. Domínguez are with the Department of Electronics, University of Valladolid, 47011 Valladolid, Spain (e-mail: sdueñas@ele.uva.es).

E. Miranda is with the Universitat Autònoma de Barcelona, 08193 Bellaterra, Spain.

Color versions of one or more of the figures in this letter are available online at <http://ieeexplore.ieee.org>.

Digital Object Identifier 10.1109/LED.2017.2723054

computation and ultradense information storage [7]–[9], but also in less explored fields including analog circuits [10], neuromorphic circuits for biological processes simulation [11], spintronics [12], etc.

The generated theoretical and experimental background about these devices has led to the proposal of similar systems in which the capacitance or inductance would depend on their previous history. They are named, respectively, memcapacitors and meminductors [13], [14]. This way, the three fundamental elements of electronic circuits, all of which are two-terminal passive devices, would be able to store information without the need of a power source. Their specific properties would appear as a hysteretic loop in two characteristic variables in each case: current-voltage for memristors, charge-voltage for memcapacitors, and current-flux for meminductors. Despite the suggestive nature of this possibility, so far a few systems have been found to operate as memcapacitors or meminductors, and hence their study has been approached from an essentially theoretical perspective [15]–[17]. A reversible non-volatile capacitance change effect was observed in perovskite oxide thin films when they were exposed to short electrical pulses [18]. Conductance changes due to vacancy motion in perovskite interface region near the electrode contact coexisted with the capacitance changes. Similar concurrent resistive and capacitive switching effect was reported in LaAlO₃ [19], VO₂ (20) and TiO₂ based solid state memristive devices [21]. Cheng *et al.* [22] reported capacitance-voltage hysteresis loops on a Ni/GeO_x/nc-TiO₂/TaON/TaN memristive device. During the set process, charged vacancies were formed near bottom TaN, resulting in high values of capacitance. During reset, injected electrons from the Ni top electrode diffused toward TaN electrode and charged vacancies were neutralized, thus giving a lower capacitance value. Qingjiang *et al.* [23] demonstrated that TiO₂-based metal-insulator-metal (MIM) devices possess resistive, capacitive and inductive components that can concurrently be programmed. Also, the impedance value tuning by adjusting both resistance and capacitance values of HfO₂ based bi-layer devices was recently reported [24].

II. EXPERIMENT

In this work we present an experimental observation of negative susceptance of TiN/Ti/20 nm-HfO₂/W MIM structures, which exhibit a bipolar resistive-switching. HfO₂ films were deposited by atomic layer deposition (ALD) at 225 °C using TDMAH and H₂O as precursors, and N₂ as carrier and purge gas. The resulting structures are square cells of 50 × 50 μm². Electrical measurements were carried out putting the sample

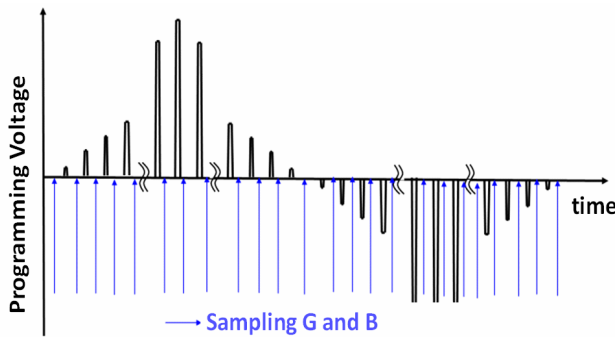


Fig. 1. Programming voltage bias sequence used to record the admittance values at 0 volts.

in a light-tight, electrically shielded box. DC-current and admittance were measured using a Keithley 4200SCS semiconductor analyzer. The voltage was applied to the TiN/Ti top electrode with the W bottom electrode grounded. To avoid the effect of parasitic elements (series resistance or inductance due to wiring, needles, etc.) a four-probe measurement setup was used. At each electrode, one probe was used to apply and measure the voltage, while the other one sensed the current. Moreover, a careful short/open calibration process to compensate potential artifacts of the experimental bench was carried out. Real and imaginary parts of the impedance lower than 4 Ω were measured in short-circuit, and higher than 10⁹ Ω in open-circuit configuration. Therefore, we can ensure that the measured values are only due to the devices under test.

III. RESULTS AND DISCUSSION

Conductive filaments (CFs) were formed on the TiN/Ti/HfO₂/W MIM capacitors when applying a voltage of around 4 V. In order to prevent irreversible dielectric breakdown a current compliance of 100 μA was used during the electroforming process. Once the CF is formed, an excellent repetitiveness was observed. The low resistive state (ON state) was achieved by applying a voltage bias of +1.2 V, and the high resistance state (OFF state) was reached when applying a negative voltage of -1.6 V. In order to study in depth the evolution of the CFs with the bias voltage, we recorded the device small-signal parameters by means of the programming voltages sequence showed in Fig. 1, in which each pulse is 1 ms-long. Admittance signal was measured at 0 V bias (in order not to modify the CFs during measurements) with a superimposed 30 mV rms-ac signal. The data acquisition instrument provides the admittance values according to the following expression:

$$Y = G + jB \quad (1)$$

Being the conductance G the phase component, and the susceptance B the quadrature component with respect to the small signal applied. Fig. 2 shows, for three frequency values, the conductance, G (a), and the susceptance over the angular frequency, B/ω (b), as a function of the programming voltage pulses height. In the OFF state, at programming voltages between -1.6 V and +0.5 V, both G and B/ω remain constant. G has a low value, as corresponds to the high resistance state (HRS), whereas B/ω is positive, thus indicating a dominant capacitive behavior. On the other hand, in the ON state

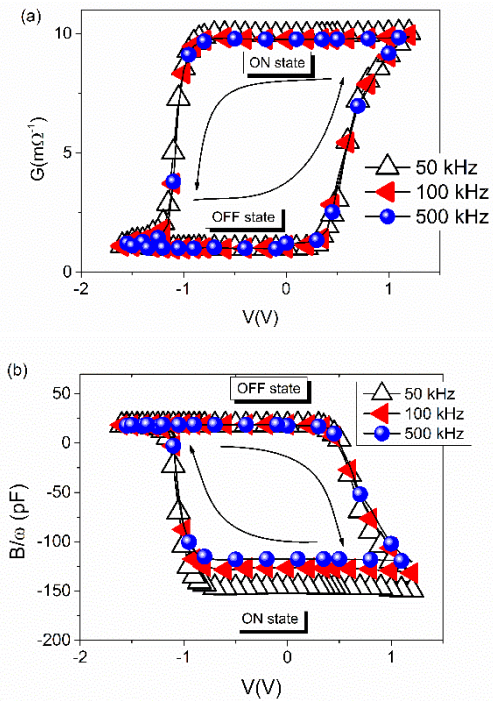


Fig. 2. Conductance (a) and susceptance (b) measured at 0 volts vs. programming voltage at three frequencies.

both magnitude remain constant at programming voltages between +1.2 V and -1 V. G has a high value, as corresponds to the low resistance state (LRS), whereas B/ω is negative, thus indicating a dominant inductive behavior. The transition from the OFF state to the ON state is not sharp, but gradual between +0.4 V and +1.2 V, in which interval the CFs are not completely built. The CFs dilution, i.e. the transition from the ON state to the OFF state, is progressive as well, especially for the G case, and takes place between -0.9 V and -1.6 V. As for B/ω , it changes from a negative value (corresponding to an inductive behavior) to a positive one (corresponding to a capacitive behavior) at around -1.0 V. Also, B/ω depends on the frequency, reaching lower values as frequency decreases. Hence, the dominant inductive behavior of the CFs disappears when CFs dilute during the transition ON → OFF. A rigorous circuit modelling of the capacitors would require an in-depth study which is beyond the scope of this work. We use a very simple three-parameter circuit model (Fig. 3) based on the one proposed by Wakrim *et al.* [24]. The CFs, that behaves as a resistance (R) in series with an inductance (L), are in parallel with the geometrical capacitance of the MIM structure (C). C is the capacitance at 0 V and at the OFF state and results to have a value of 22 pF, corresponding to a permittivity value of the HfO₂ film of $K=20$. In the ON state R exhibits a low value, whereas L value is appreciable. When the device switches to the OFF state, CFs become partially diluted so that R increases and L decreases. The high value of the inductance L observed at the ON state, has not to be interpreted in terms of the self-inductance of the filaments, which are only 20 nm long. Instead, we suggest that the measured inductance could be originated by transport mechanisms which make current lag behind the electric field. These mechanisms include hopping conduction between connected oxygen vacancies [24], charge trapping on defects existing at the interface between the filaments and the surrounding dielectric, space-charge-limited

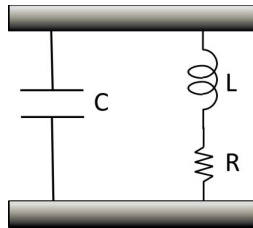


Fig. 3. Three parameter equivalent circuit for the MIM capacitors.

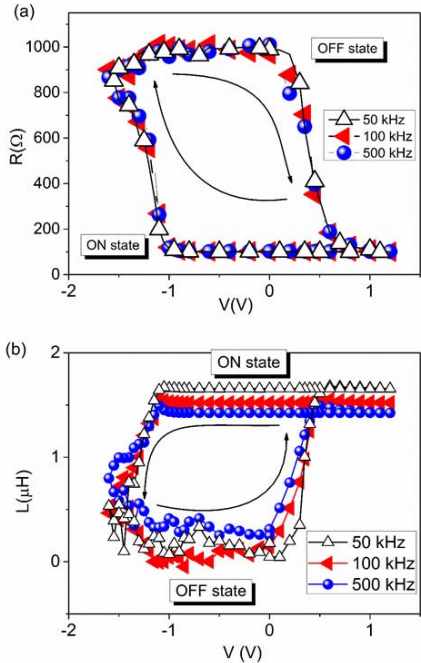


Fig. 4. Resistance (a) and inductance (b) of the conductive filaments vs programming voltage.

current (SCLC) [25], etc. Future work is needed to determine the very nature of the negative susceptance.

The total admittance of the structure can be expressed as:

$$Y = \frac{1}{R + j\omega L} + j\omega C \quad (2)$$

and the real and imaginary parts of Y read:

$$\text{Real}(Y) = G = \left(\frac{1}{R}\right) \frac{1}{1 + \frac{\omega^2 L^2}{R^2}} \quad (3)$$

$$\text{Im}(Y) = B = \omega \left(C - \frac{L/R^2}{1 + \omega^2 L^2/R^2}\right) \quad (4)$$

In these expressions, L affects both the real and imaginary parts of the admittance. In particular, the existence of an inductive component reduces the susceptance value, which can reach negative values (Eq. 4) when $\left(\frac{L/R^2}{1 + \omega^2 L^2/R^2}\right) > C$.

From experimental results of Fig. 2, and by using Equations (3) and (4), the variations of R and L with the programming voltage were obtained (Fig. 4). The evolution from the OFF state to the ON state is observed from positive values slightly above 0 V, when R starts to decrease and L starts to increase. When positive voltage is applied the density of oxygen vacancies gradually increases. On average, the distance between vacancies diminishes, hence more conductive paths

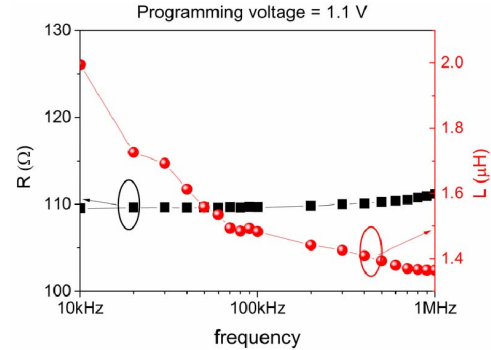


Fig. 5. Frequency dependence of the resistance and inductance at 0 volts of the conductive filaments after a programming voltage of 1.1 volts.

are formed. R and L reach their saturation values at around $+0.5$ V, thus indicating that the CFs are already fully built and the top and bottom electrodes are interconnected. From voltage values higher than $+0.5$ V, R value continues diminishing, which would indicate that the average distance between oxygen vacancies diminishes or new CFs are being created. On the other hand, in the ON state to the OFF state transition, L remains constant, and so the CFs remain unchanged, until a negative voltage value of around -1 V is applied. So, it is necessary a programming voltage of at least -1 V to activate the motion of oxygen atoms which lead to the CFs oxidation, i.e., their dissolution. As for the frequency dependency of R and L parameters, Fig. 5 depicts their variation in the ON state and at a programming voltage of $+1.1$ V, between 10 kHz and 1 MHz. The resistance slightly raises, whereas the inductance clearly diminishes when frequency increases. This could be explained considering that as frequency increases, the period of the applied a.c. signal approaches to the time constants of the transport mechanisms causing the lag between current and electric field.

IV. CONCLUSION

In summary, in this work we show that RRAM devices show two clearly separated values in the imaginary part of the admittance (susceptance). In the ON state the susceptance is negative. An inductive term appears due to delays between the current through the filaments and the applied voltage caused by transport mechanisms. The physical nature of these mechanisms is out of the scope of this work and need future study. In the OFF state the inductive term disappears and the susceptance only consists on the geometrical capacitance of MIM structure. It is also shown that the HRS to LRS transition starts for positive voltages near 0 V due to the formation of oxygen-vacancy conductive paths. The inductance reaches a saturation value at around $+0.5$ V, which indicates that from this programming voltage values the CFs completely extend between the top and bottom electrodes. Further increasing of voltage reinforces the CFs and/or gives rise to the generation of new CFs. On the other hand, the LRS to HRS transition requires programming voltages of the order of -1 V to oxidize the oxygen vacancies clusters which make up the CFs.

ACKNOWLEDGMENT

Authors would like to acknowledge Prof. Campabadal group from the Institute of Microelectronics of Barcelona (IMB-CSIC, Spain) for providing the samples of this study.

REFERENCES

- [1] D. Ielmini, "Resistive switching memories based on metal oxides: Mechanisms, reliability and scaling," *Semicond. Sci. Technol.*, vol. 31, p. 063002, May 2016, doi: 10.1088/0268-1242/31/6/063002.
- [2] S. L. Barbera, D. Vuillaume, and F. Alibart, "Filamentary switching: Synaptic plasticity through device volatility," *ACS Nano*, vol. 9, no. 1, pp. 941–949, 2015, doi: 10.1021/nn506735m.
- [3] S. Brivio, E. Covi, A. Serb, T. Prodromakis, M. Fanciulli, and S. Spiga, "Experimental study of gradual/abrupt dynamics of HfO₂-based memristive devices," *Appl. Phys. Lett.*, vol. 109, p. 133504, Sep. 2016, doi: 10.1063/1.4963675.
- [4] G. Niu, P. Calka, M. A. der Maur, F. Santoni, S. Guha, M. Fraschke, P. Hamoumou, B. Gautier, E. Perez, C. Walczyk, C. Wenger, A. D. Carlo, L. Alff, and T. Schroeder, "Geometric conductive filament confinement by nanotips for resistive switching of HfO₂-RRAM devices with high performance," *Sci. Rep.*, vol. 6, p. 25757, May 2016, doi: 10.1038/srep25757.
- [5] L. Chua, "Memristor—The missing circuit element," *IEEE Trans. Circuit Theory*, vol. 18, no. 5, pp. 507–519, Sep. 1971, doi: 10.1109/TCT.1971.1083337.
- [6] L. O. Chua and S. M. Kang, "Memristive devices and systems," *Proc. IEEE*, vol. 64, no. 2, pp. 209–223, Feb. 1976, doi: 10.1109/PROC.1976.10092.
- [7] Y. Watanabe, J. G. Bednorz, A. Bietsch, C. Gerber, D. Widmer, A. Beck, and S. J. Wind, "Current-driven insulator-conductor transition and non-volatile memory in chromium-doped SrTiO₃ single crystals," *Appl. Phys. Lett.*, vol. 78, no. 23, pp. 3738–3740, Jun. 2001, doi: 10.1063/1.1377617.
- [8] M. J. Rozenberg, I. H. Inoue, and M. J. Sánchez, "Nonvolatile memory with multilevel switching: A basic model," *Phys. Rev. Lett.*, vol. 92, no. 17, p. 178302, Apr. 2004, doi: 10.1103/PhysRevLett.92.178302.
- [9] C. Yoshida, K. Tsunoda, H. Noshiro, and Y. Sugiyama, "High speed resistive switching in Pt/TiO₂/TiN film for nonvolatile memory application," *Appl. Phys. Lett.*, vol. 91, p. 223510, Nov. 2007, doi: 10.1063/1.2818691.
- [10] Y. V. Pershin and M. D. Ventra, "Practical approach to programmable analog circuits with memristors," *IEEE Trans. Circuits Syst. I, Reg. Papers*, vol. 57, no. 8, pp. 1857–1864, Aug. 2010, doi: 10.1109/TCSI.2009.2038539.
- [11] Y. V. Pershin, S. L. Fontaine, and M. D. Ventra, "Memristive model of amoeba learning," *Phys. Rev. E, Stat. Phys. Plasmas Fluids Relat. Interdiscip. Top.*, vol. 80, p. 021926, Jan. 2009, doi: 10.1103/PhysRevE.80.021926.
- [12] Y. V. Pershin and M. D. Ventra, "Spin memristive systems: Spin memory effects in semiconductor spintronics," *Phys. Rev. E, Stat. Phys. Plasmas Fluids Relat. Interdiscip. Top.*, vol. 78, p. 113309, Sep. 2008, doi: 10.1103/PhysRevB.78.113309.
- [13] M. D. Ventra, Y. V. Pershin, and L. O. Chua, "Putting memory into circuit elements: Memristors, memcapacitors, and meminductors," *Proc. IEEE*, vol. 97, no. 8, pp. 1371–1372, Aug. 2009, doi: 10.1109/JPROC.2009.2022882.
- [14] M. D. Ventra, Y. V. Pershin, and L. O. Chua, "Circuit elements with memory: Memristors, memcapacitors, and meminductors," *Proc. IEEE*, vol. 97, no. 10, pp. 1717–1724, Oct. 2009, doi: 10.1109/JPROC.2009.2021077.
- [15] Y. V. Pershin and M. D. Ventra, "Memristive circuits simulate memcapacitors and meminductors," *Electron. Lett.*, vol. 46, no. 7, pp. 517–518, Apr. 2010, doi: 10.1049/el.2010.2830.
- [16] J. Martinez-Rincon, M. D. Ventra, and Y. V. Pershin, "Solid-state memcapacitive system with negative and diverging capacitance," *Phys. Rev. B, Condens. Matter*, vol. 81, p. 195430, May 2010, doi: 10.1103/PhysRevB.81.195430.
- [17] Y. V. Pershin, V. A. Slipko, and M. D. Ventra, "Reconfigurable transmission lines with memcapacitive materials," *Appl. Phys. Lett.*, vol. 107, p. 253101, Dec. 2015, doi: 10.1063/1.4937808.
- [18] S. Liu, N. Wu, A. Ignatiev, and J. Li, "Electric-pulse-induced capacitance change effect in perovskite oxide thin films," *J. Appl. Phys.*, vol. 100, no. 5, p. 056101, Sep. 2006, doi: 10.1063/1.2337387.
- [19] S. X. Wu, H. Y. Peng, and T. Wu, "Concurrent nonvolatile resistance and capacitance switching in LaAlO₃," *Appl. Phys. Lett.*, vol. 98, no. 9, p. 093503, Feb. 2011, doi: 10.1063/1.3560257.
- [20] T. Driscoll, H.-T. Kim, B.-G. Chae, B.-J. Kim, Y.-W. Lee, N. M. Jokerst, S. Palit, D. R. Smith, M. D. Ventra, and D. N. Basov, "Memory metamaterials," *Science*, vol. 325, pp. 1518–1521, Feb. 2009, doi: 10.1126/science.1176580.
- [21] I. Salaoru, A. Khiat, Q. Li, R. Berdan, and T. Prodromakis, "Pulse-induced resistive and capacitive switching in TiO₂ thin film devices," *App. Phys. Lett.*, vol. 103, p. 233513, Dec. 2013, doi: 10.1063/1.4840316.
- [22] C. H. Cheng, P. C. Chen, Y. H. Wu, and A. Chin, "Long-endurance nanocrystal TiO₂ resistive memory using a TaON buffer layer," *IEEE Electron Device Lett.*, vol. 32, no. 12, pp. 1749–1751, Dec. 2011, doi: 10.1109/LED.2011.2168939.
- [23] L. Qingjiang, A. Khiat, I. Salaoru, C. Papavassiliou, X. Hui, and T. Prodromakis, "Memory impedance in TiO₂ based metal-insulator-metal devices," *Sci. Rep.*, vol. 4, p. 4522, Mar. 2014, doi: 10.1038/srep04522.
- [24] T. Wakrim, C. Vallée, P. Gonon, C. Mannequin, and A. Sylvestre, "From MEMRISTOR to MEMImpedance device," *Appl. Phys. Lett.*, vol. 108, no. 5, p. 053502, Feb. 2016, doi: 10.1063/1.4941231.
- [25] S. W. Tsang, S. K. So, and J. B. Xu, "Application of admittance spectroscopy to evaluate carrier mobility in organic charge transport materials," *J. Appl. Phys.*, vol. 99, no. 1, p. 013706, 2006, doi: 10.1063/1.2158494.